



Use of AFM technique to study the nano- silica effects in concrete mixture

Behdash Amiri¹, Ali Bahari², Aref Sadeghi Nik³, Adel Sadeghi Nik⁴ and Naser Salman Movahedi⁵

¹Young Researchers Club, Roudehen Branch, Islamic Azad University, Roudehen, Iran.

²Dept. of Physics, University of Mazandaran, Babolsar 47416- 1467, Iran.

^{3, 4}Young Researchers Club, Jouybar Branch, Islamic Azad University, Jouybar, Iran.

⁵Young Researchers Club, Roudehen Branch, Islamic Azad University, Roudehen, Iran.
BehdashAmiri.i@gmail.com¹; a.bahari@umz.ac.ir²

Abstract

Nano structural properties of concrete can be studied with considering the variations of the nano silica/Si ratio, the silicate structure, and the contents of Si-OH in the mixture using X- Powder method, AFM (Atomic Force Microscopy) and X- Ray Diffraction (XRD) techniques. We have thus synthesized the nano silica particles by employing sol- gel method. The obtained results are led to a new aspect of the silicate - hydrate, which helps to establish quantitative relations between the nano structure and bulk properties.

Keywords: Nanotechnology, Concrete, Nano silica and AFM technique.

Introduction

The crystalline phase changes in the mechanical properties of concrete have been the subject of extensive research over the past century (Hatt, 1907; Alizadeh *et al.*, 2007). In particular, synthesizing silica nano particles in cement matrix has received significant attention due to its practical implications. Although numerous studies have been conducted in this regard, the effects of nano silica on the mechanical stability of cement-based systems is still not clearly resolved and understood. On the other hand, the combination of theory and novel experiments provide tools, whose impact on models is just being appreciated. Among these approaches, some new hypotheses proposed for describing possible mechanisms for the temporal deformation of hardened concrete under load (Bažant *et al.*, 1997; Tamtsia & Beaudoin, 2000.). Moreover, as we know all typical concrete consist of ordinary Portland cement, fillers such as coarse aggregates, admixtures and water. In cement chemistry CaO, SiO₂ and H₂O are represented by calcium and silicate hydrate, respectively. This cement that forms up to about 60% by volume of the paste, is held together by a calcium silicate hydrate (C-S-H) phase; which are formed stoichiometry and considered as the principal binding agent in the cement paste.

Many researchers (Richardson *et al.*, 2010; Alizadeh *et al.*, 2011) have believed that C- S- H is generally nearly amorphous and so difficult to characterize and displays tremendous variation in chemical composition, nanostructure, and morphology (Jennings *et al.*, 2008; Morgen *et al.*, 2009; Taylor *et al.*, 2010). These different C - S - H morphologies as revealed in AFM images and topography patterns result in different pore structures, which explains some of the differences in physical properties reported in the literature between neat Portland cement pastes and blends containing supplementary cementing materials. This approach gives

a more concrete picture than the principal bending agent in the crystallite cement paste (Bahari *et al.*, 2005; Girao *et al.*, 2010; Moudrakovski *et al.*, 2010). It is thus necessary to understand the nature of C- S- H and their phases with using XRD technique and find their morphology and atom's arrangement and distinguish the mechanisms of its degradation with AFM technique and X- Powder, topography methods.

Therefore, since concrete can deteriorate through a variety of chemical and physical processes, we have to find the crystalline phases and determine the accurate size of nano particles. We have studied the hardened cements and concretes can be considered as complex multi-phase composite materials with using XRD and AFM techniques. The obtained results indicate the effects of nano silica particles in concrete mixture yield a more mechanical stable structure of present cement mixture.

Experimental procedure and details

The sol-gel process is a wet-chemical technique (chemical solution deposition) widely used recently in the fields of materials science and ceramic engineering. Such methods are used primarily for the fabrication of materials starting from a chemical solution which acts as the precursor for an integrated network (or gel) of either discrete particles or network polymers. Typical precursors are silica oxides, which undergo various forms of hydrolysis and poly condensation reactions.

Thus, the sol evolves towards the formation of a gel-like diphasic system containing both a liquid phase and solid phase whose morphologies range from discrete particles to continuous polymer networks. In this process, calcium carbonate powder (1·16 g) was dissolved in de-ionized water to which were added citric acid crystals (0·38 g). The mixture was then stirred carefully using a magnetic stirrer while ammonium hydroxide was added to obtain a pH of 7. The mixture was then heated in a



Scheme 1. Flowchart of synthesis silica nano particles

TEOS/EtOH/HCl/H ₂ O at RT stirring for 0.5h, pH 3
TIOT/EtOH/CH ₃ COOH/ H ₂ O at RT stirring for 0.5h, pH 3
Mixing TEOS and TIOT at RT stirring for 0.5h, pH 3
CaCO ₃ .3H ₂ O / H ₂ O at RT stirring for 0.5h, pH 2
Mixing TEOS and TIOT.3H ₂ O. at RT stirring for 48h, pH 3

furnace to a temperature of 50°C for 20 h. Initially a zero gel and finally a powder were obtained.

The powder was then heated to a temperature of 80°C for 24 h to obtain a pale yellow powder. The characterization of nano silica in concrete and/or cement synthesized by the sol - gel citration method was studied by using XRD and AFM techniques. It is worth noting that the samples are cleaned inside the ultrasonic bath after rinsing and washing in heated acetone then ethanol the surface cleanliness is checked with AFM technique. Powder is synthesized via simple sol - gel method as summarized in Scheme 1. The nano -silica is also synthesised with the same procedure of CaO nano - particles based on a SiO₂ precursor.

Fig.1-3 show AFM images of samples. As shown in these images and topography spectra in Fig. 4, nanoparticles affect the concrete structures in that sample form polyhedron agglomerates and the other phases like tetrahedral as confirmed with XRD pattern in Fig. 5.

The AFM images and topography spectra from the specimens, show mudflat cracking throughout an otherwise smooth and flat coherent surface layer covering the nano bulk structures with silica nano particles. Higher magnification imaging in these figures reveals that concrete spans these cracks and appears to stabilize the surface layer against creep and stress relaxation of cement - based materials and formed the viscoelastic repose of C- S- H, as indicated in topography.

XRD technique is also used for crystal phase identification and estimation of the crystallite size. XRD patterns were measured on a (GBC-MMA 007 (2000)) X-ray diffractometer. The diffractograms were recorded with 0.02° step size in where the speed was 10 deg/min

$10 \frac{\text{deg}}{\text{min}}$ radiation over a 2θ range of 10° - 90° at a sampling width of 0.2° and a scanning speed of 10 deg/min. The XRD patterns of samples compose calcined at different temperatures. The crystalline peaks corresponded to silica in the form of either highly pure (001) phase or mixed (002), (022) and (004), except the as - prepared nanostructure showing amorphous phase. This point indicates that increase in crystalline phase transformation of sample peak place when the amount of silica nanoparticles (10%) in concrete content is added. The range of nano particle size is between 31 nm to 150 nm as shown in Fig.6.

Discussion

It is well-known that XRD sensitivity to detect crystalline phases depends on their concentration and their crystallite size when it is extremely small. A very small crystallite size produces diffraction peaks so wide that the diffraction pattern of its phase, when it appears in a low concentration, can be lost in background.

Data were acquired over the range of 2θ from 10 to 90° indicate the change of crystalline structure. Figure 5 illustrates the XRD patterns of samples. From the figure, it was found that all the films were polycrystalline having silica phase. It is observed that the sample exhibited characteristic peaks of austenite crystal plane (001), (002), (022) and (004). Crystallite size, lattice microstrain and lattice parameter of each alloy powder has calculated from the XRD peak broadening. Following Scherrer equation, the crystallite sizes have been determined for samples (Bahari *et al.*, 2006; Bahari *et al.*, 2006).

$$\Gamma = \frac{K \lambda}{\beta \cos \theta}$$

Where Γ , K , λ , β and θ is mean crystallite dimension, x-ray wavelength, FWHM (in radians) and Bragg angle, respectively.

The crystallite size estimated from the XRD analysis of the powder was close to 30 nm. This suggests that major structural changes and dissolution of the alloying elements almost completed by 20 h. This is because of the entrance of silica atoms into the lattice of the concrete which changes distortion structure to amorphous structure in it.

Finally, after 20h of heating a finer refined structure has obtained. It shows a homogeneous chemical composition has obtained for sample heated for 20 h. Moreover, the surface area and density of nano silica particles are demonstrated AFM images with different forms.

As shown in these Fig.1-6, the C-S-H bonds are naturally formed in the sol - gel processes due to reaction between amorphous SiO₂ and CaO in excess water (water/solid ratio by mass ≈ 10), in that reactive silica heated at 60 °C. Calcium oxide was obtained from the calcinations of the reagent grade calcium carbonate at 80 °C and were prepared using stoichiometric amounts of CaO and SiO₂ resulting in C/S ratios of 0.8, 1.2 and 1.5. Distilled de-aired water was added to the dry mixture of CaO and SiO₂ in 1 L bottles. The bottles were mounted on a magnetic stirrer and the reaction continued for 2 days.

Conclusion

In the present work we found that the thickness of the compacted C-S-H samples varied between 0.8 and 1.2 mm depending on the C/S ratio. It is suggested that the monolayer of water present on the surface of particles before compaction may have moved to 'pore' spaces after the particles come into contact in the compacted

sample. Excess water in the pores is then removed during heating the sample. We also found in this paper,

Fig.1 - 2D . AFM image of with (top) and without (bottom) nano silica particles in concrete content. Maanification: X 2500.

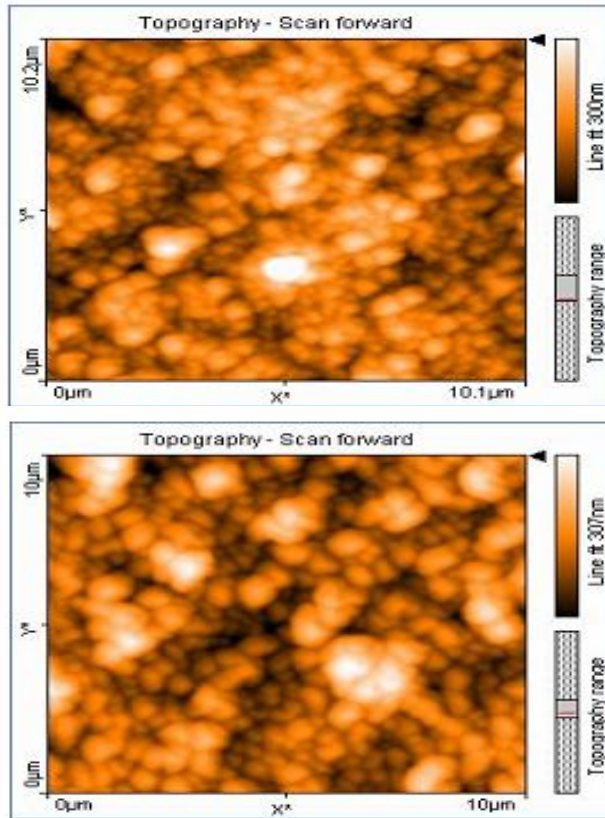


Fig.2 - 2D . AFM image of with (top) and without (bottom) nano silica particles in concrete content. Magnification: X 1000.

Fig.3- 3D . AFM image of without (top) and with (bottom) nano silica, in concrete content. Magnification: X 1000

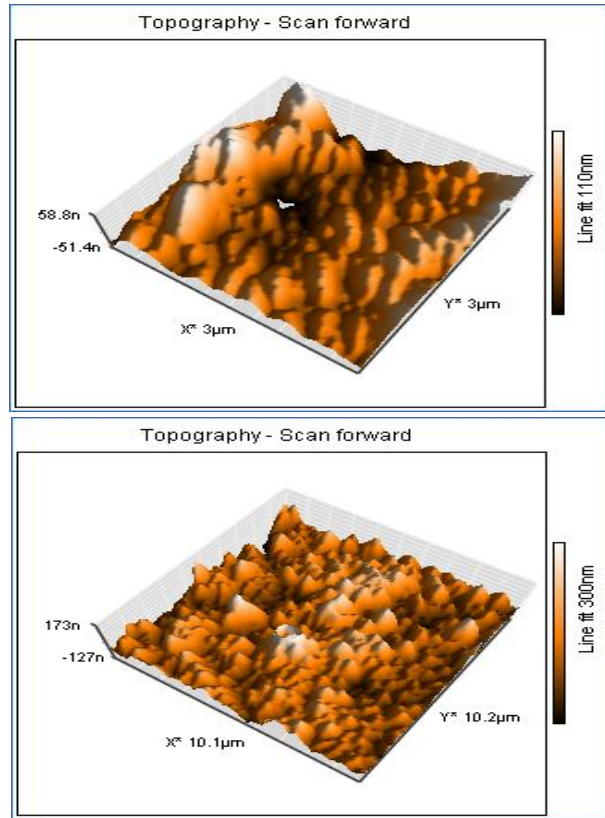


Fig.4 - 2D . Topography spectra of concrete: without nano silica (top) and with (bottom) nano silica particles.

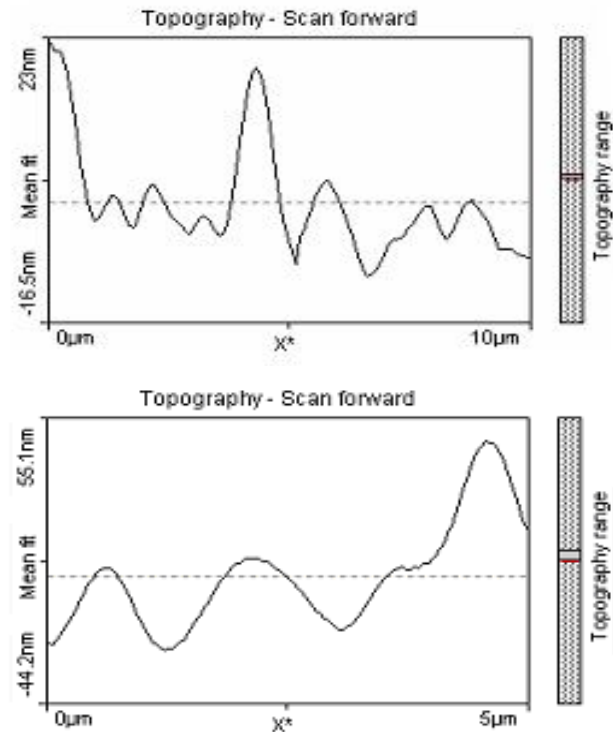
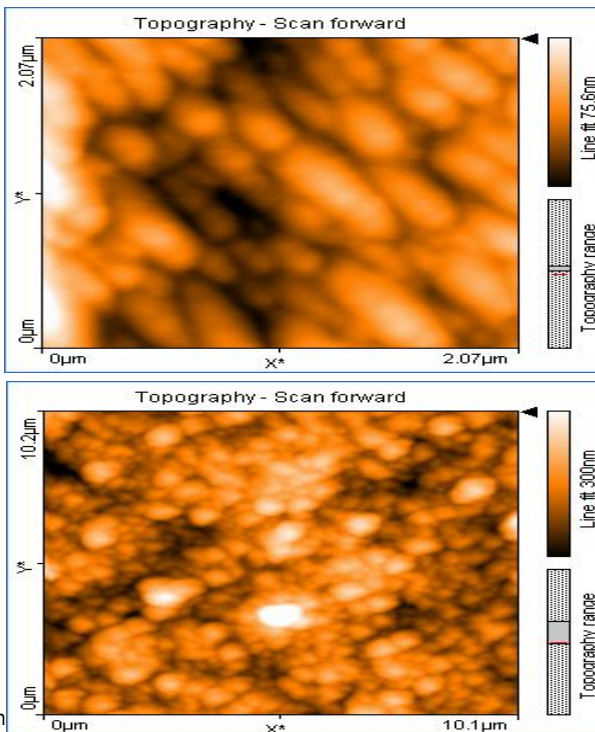


Fig.5. XRD pattern of nano silica in cement matrix

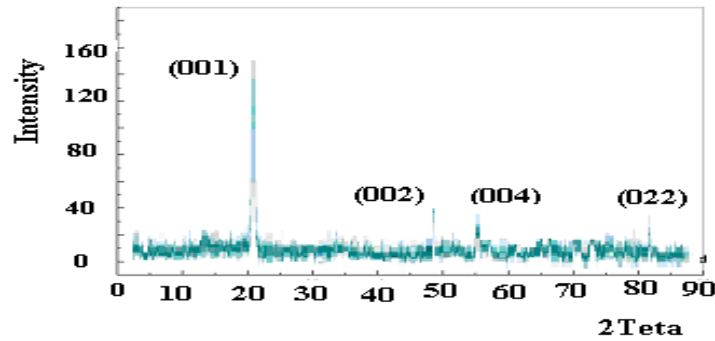
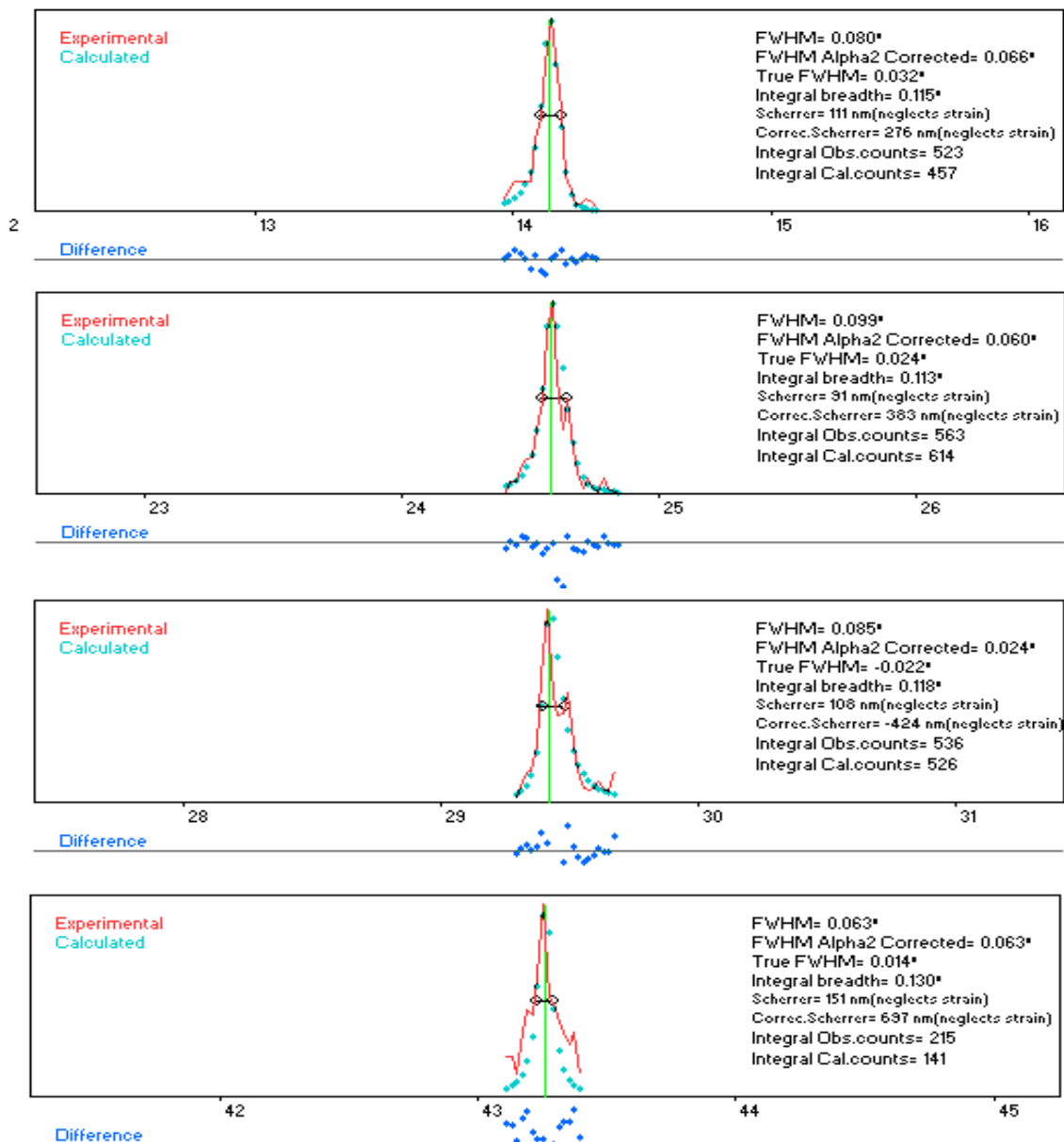


Fig.6. The size of nanoparticles correspond with Fig.5, are determined with using X- Powder method





the omission of bridging tetrahedral and further defects in the nano silica - cement chain in addition to the presence of calcium ions in the interlayer region can accommodate a variety of compositional changes for C- S- H systems as are revealed in AFM images, XRD, X- Powder and topography methods.

Acknowledgements

We would like to thank the Young Researchers Club, Roudehen Branch, Islamic Azad University, Roudehen, Iran for financial support.

References

1. Alizadeh R, Beaudoin JJ and Raki L (2007) C-S-H (I) - a nanostructural model for the removal of water from hydrated cement Paste. *J. Am. Ceram Soc.* 90 (2), 670-672.
2. Alizadeh R, Beaudoin JJ, Raki L, Terskikh V (2011) C-S-H/Polyaniline nanocomposites prepared by *in situ* polymerization. *J. Mat. Sci.* 46, 460-467.
3. Bahari A, Li ZS and Morgen P (2006) Valence band studies of the formation of ultrathin pure silicon nitride film on Si(100), *Surf. Sci.* 600, 2966.
4. Bahari A, Morgen P, Pederson K and Li Z (2006) Growth of a stacked silicon nitride / silicon oxide dielectric on Si(100), *J. Vac. Sci. Technol. B*, 24, 2119.
5. Bahari A, Robenhagen U, Morgen P and Li Z (2005) Growth of ultrathin silicon nitride on Si(111) at low temperature. *Phys. Rev. B*, 72, 205323.
6. Bažant ZP, Hauggaard AB, Baweja S and Ulm F- J (1997) Microprestress- solidification theory for concrete creep. I: aging and drying effects. *J. Eng. Mech.* 123 (11), 1188-1194.
7. Girao AV, Richardson IG, Taylor R, Brydson RMD (2010) Composition, morphology and nanostructure of C-S-H in 70% white Portland cement-30% fly ash blends hydrated at 55 degrees C. *Cem. Concr. Res.* 40, 1350-1359.
8. Hatt WK (1907) Notes on the effect of time element in loading reinforced concrete beams. *Proc. Am. Soc. Test Mater.* 7, 421-433.
9. Jennings HM (2008) Refinements to colloid model of C-S-H in cement: CM-II. *Cem. Concr. Res.* 38, 275-289.
10. Morgen P, Bahari A, Pederson K and Li Z (2009) Plasma assisted growth of ultrathin nitrides on Si surfaces under ultrahigh vacuum condition. *J. Physics Conf.* 86, 01200.
11. Moudrakovski I, Alizadeh R and Beaudoin JJ (2010) Natural abundance ultra-high field ^{43}Ca solid state NMR of cement-based materials. *Phys. Chem. Chem. Phys.* 12, 6961-6969.
12. Richardson IG, Skibsted J, Black L and Kirkpatrick RJ (2010) Characterisation of cement hydrate phases by TEM, NMR and Raman spectroscopy. *Adv. in Cem. Res.* 22, 233-248.
13. Tamtsia BT and Beaudoin JJ (2000) Basic creep of hardened cement paste - a re-examination of the role of water. *Cem. Concr. Res.* 30, 1465-1475.
14. Taylor R, Richardson IG, Brydson RMD, (2010) Composition and microstructure of 20-year-old ordinary Portland cement-ground granulated blast-furnace slag blends containing 0 to 100% slag. *Cem. Concr. Res.* 40, 971-983.